

Inner Core Differential Motion Confirmed by Earthquake Waveform Doublets

Jian Zhang,^{1*} Xiaodong Song,^{2*†} Yingchun Li,² Paul G. Richards,¹
Xinlei Sun,² Felix Waldhauser¹

We analyzed 18 high-quality waveform doublets with time separations of up to 35 years in the South Sandwich Islands region, for which the seismic signals have traversed the inner core as *PKP(DF)*. The doublets show a consistent temporal change of travel times at up to 58 stations in and near Alaska, and they show a dissimilarity of *PKP(DF)* coda. Using waveform doublets avoids artifacts of earthquake mislocations and contamination from small-scale heterogeneities. Our results confirm that Earth's inner core is rotating faster than the mantle and crust at about 0.3° to 0.5° per year.

The Earth's inner core plays an important role in the geodynamo that generates the Earth's magnetic field, and an electromagnetic torque from the geodynamo is expected to drive the inner core to rotate relative to the mantle and crust (1–3). Song and Richards (4) analyzed seismic waves traversing the Earth's fluid and solid cores and reported evidence for a differential inner core rotation. They found that differential travel times between the *BC* and *DF* branches of *PKP* waves (Fig. 1) along the

pathway from earthquakes in the South Sandwich Islands (SSI) to a seismic station at College, Alaska (COL), increased systematically by about 0.3 s from 1967 to 1995. The temporal change was interpreted first as a change of the orientation of the fast axis of the inner core anisotropy (4), but later and preferably as a shift of lateral velocity gradient in the inner core (5, 6) caused by the inner core rotation. Subsequent studies have provided further support (5–15), and most estimates of the rotation rate are a few tenths of a degree per year faster than the rotation of the Earth (a super-rotation). However, some studies have failed to resolve a nonzero rotation (16, 17), and claims of a travel-time change have been challenged as artifacts (18–21).

Waveform doublets can potentially provide much stronger evidence of temporal change

by avoiding artifacts of event mislocation and contamination from heterogeneities (Fig. 1, B and C). A waveform doublet is a pair of earthquakes occurring at essentially the same spatial position, as evidenced by their highly similar waveforms at each station recording both events (22). Such ideal waveform doublets are commonly found among small earthquakes (22, 23) but are rare for earthquakes large enough to generate *PKP* signals clearly. The high similarity of *BC* and *AB* signals in our doublets is due to propagation paths outside the inner core that sample the same heterogeneities. Observed differences in *DF* give information on changes in the inner core.

Poupinet *et al.* (20) developed a method to use pairs of SSI earthquakes to detect inner core rotation, but the earthquake pairs they used were not waveform doublets (24). Li and Richards (12) reported a waveform doublet in the SSI region (one event in 1987 and the other in 1995), which had clear but weak *DF* signals at the station COL, showing a time shift of 0.10 to 0.15 s in *DF* over 8.5 years. Here, we report observations of 17 additional waveform doublets in the SSI region separated by up to 35 years and detected at up to 58 stations (fig. S1). These doublets show systematic changes in *DF* travel times and coda waveforms, providing strong support for differential inner core rotation.

Waveforms of all the 18 doublets are shown in Fig. 2 and figs. S2 to S6, which are derived from 30 earthquakes that occurred from 1961 to 2004 (tables S1 and S2) (25). The *BC* and *AB* waveforms of these event pairs at COL and Beaver Creek array stations (BC01 and BC04) are highly similar (Fig. 2A), with cross-correlation coefficients of 0.79 to 0.99 (table

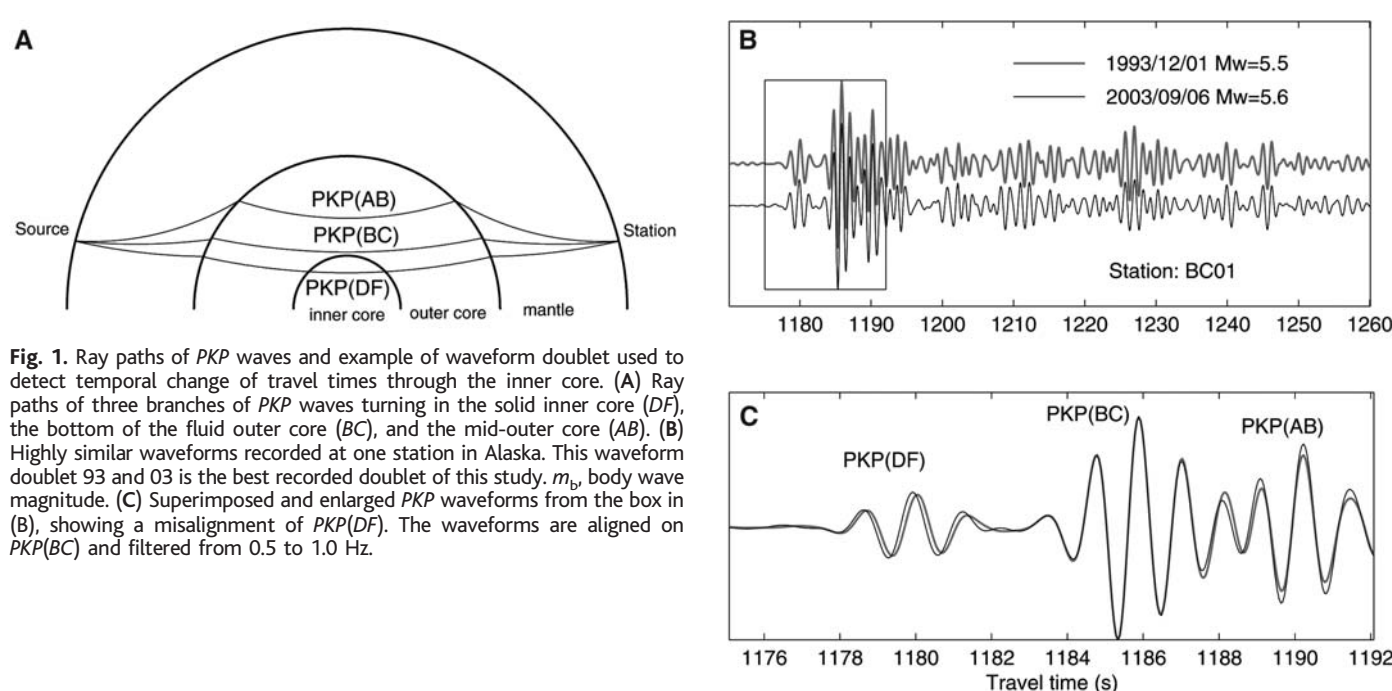


Fig. 1. Ray paths of *PKP* waves and example of waveform doublet used to detect temporal change of travel times through the inner core. (A) Ray paths of three branches of *PKP* waves turning in the solid inner core (*DF*), the bottom of the fluid outer core (*BC*), and the mid-outer core (*AB*). (B) Highly similar waveforms recorded at one station in Alaska. This waveform doublet 93 and 03 is the best recorded doublet of this study. m_b , body wave magnitude. (C) Superimposed and enlarged *PKP* waveforms from the box in (B), showing a misalignment of *PKP(DF)*. The waveforms are aligned on *PKP(BC)* and filtered from 0.5 to 1.0 Hz.

S2). Such waveform similarity allows us to measure relative time shifts with high precision. We measured the relative time shifts of the three phases (i.e., *DF* with *DF*, *BC* with *BC*, and *AB* with *AB*) by time-domain waveform cross correlation. The difference in differential *BC* – *DF* times, $d(BC - DF)$, and the difference in differential *AB* – *BC* times, $d(AB - BC)$, are then derived from the relative shifts of the three phases (table S2). The $d(AB - BC)$ value of each event pair varies from 0.0 to 0.09 s, indicating a difference in epicentral distance of less than 5.5 km (from a standard reference Earth model). Additional stations show similarity of waveforms for 16 of the 18 pairs (fig. S6 and table S2).

When signals from these high-quality waveform doublets are aligned on the *BC* phase, the *DF* phases for event pairs with time separation of less than 4 years overlap with each other well; however, the *DF* phase of the later event arrives consistently earlier than that of the earlier event for doublets separated by more than 4 years, and the *DF* phase is seen to arrive progressively earlier as the time separation increases (Fig. 2B). Also, the waveforms of the *DF* coda become dissimilar when the time separation is larger than 7 to 10 years.

The best recorded example is doublet 93 and 03 [1 December 1993, body wave magnitude (m_b) 5.5; and 6 September 2003, m_b 5.6] (Fig. 1 and figs. S4 and S5). We obtained waveform records for both events at 102 stations distributed over a large range of distances and azimuths. The cross-correlation coefficient is higher than 0.9 for short-period waveforms in a 180-s-long window at most of these stations. A double-difference analysis (26) with the use of catalog and hand-picked arrival times and relative travel times from waveform correlation shows the two events are within 1 km horizontally and about 100 m vertically (fig. S7) (25). Among the 102 stations, 58 of those in and near Alaska (fig. S1 and table S3) recorded clear *DF* signals. The *DF* amplitudes are particularly strong at Beaver Creek array (fig. S4). The directly observed values of $d(BC - DF)$ are positive for all the 58 stations, which is strong evidence for change in the inner core occurring somewhere along the paths shown in Fig. 3. The doublet was recorded by four arrays at a total of 35 stations (table S3), which can be used to estimate empirically the effect of small mislocation on $d(BC - DF)$ times (fig. S8) (25). Our analysis using Eileson array data shows that the effect of plausible mislocation of ~ 1 km is far too small (about 0.013 s) to cause the observed $d(BC - DF)$ of about 0.1 s (Fig. 3B and table S3). If we use a reference Earth model, the effect is even smaller.

The change in $d(BC - DF)$ between time $T + \Delta T$ and time T can be expressed to first order as $d(BC - DF) = \frac{\Delta v}{v_0} t_0$, where $\frac{\Delta v}{v_0}$ is the

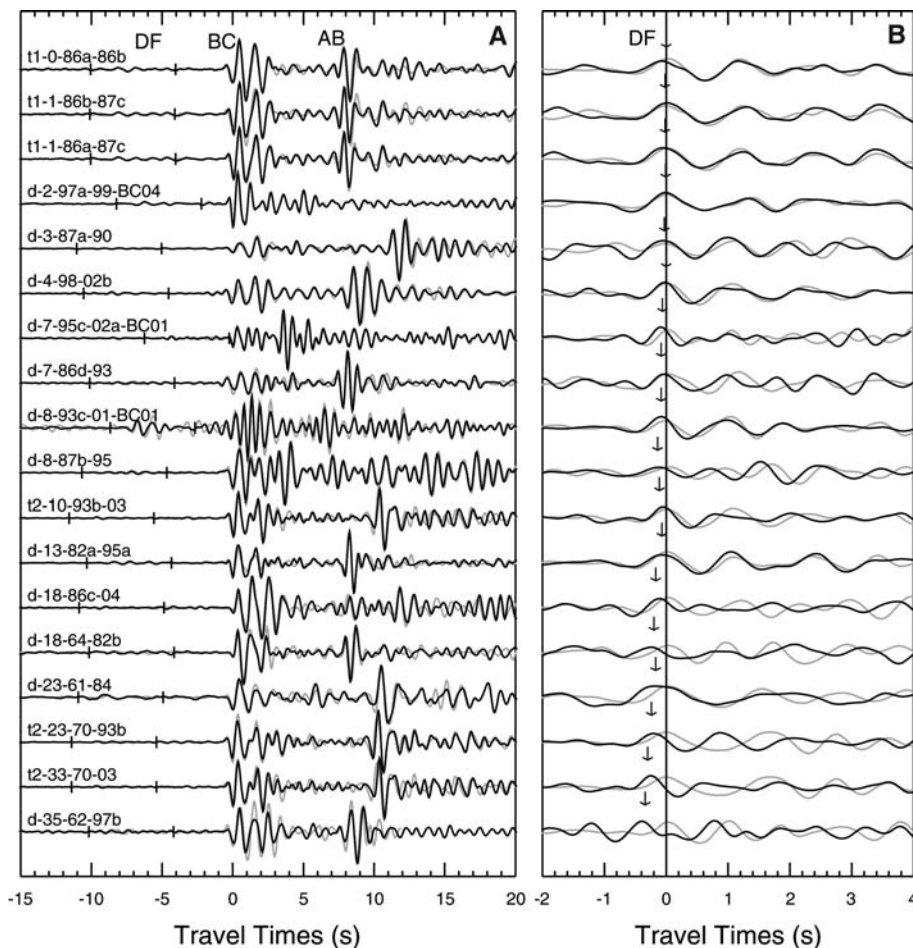


Fig. 2. (A) PKP waveforms at COL station and Beaver Creek array stations BC01 and BC04 of 17 SSI doublets found in this study and one discovered previously (12). The traces (gray for the earlier event, black for the later one) are aligned with the *BC* phase. They are sorted with increasing time separation from top to bottom (the year difference and the years of the two events are indicated in the label). **(B)** Enlarged view of *DF* segments marked by ticks in (A). The traces have been shifted so that the onset of the *DF* arrival of the earlier event of each doublet is roughly aligned. The arrow marks the measured difference of *BC* – *DF* times (table S2).

fractional inner core velocity change over the time period ΔT averaged along the ray path in the inner core, and t_0 and v_0 are the travel time and velocity in the inner core for a reference Earth model, respectively. The fractional change in inner core velocity, $\frac{\Delta v}{v_0} = \frac{d(BC - DF)}{t_0}$, inferred from the doublets that are separated by more than 4 years is $0.089 \pm 0.031\%$ (\pm SD) over 10 years (Fig. 3B). The temporal change in inner core velocity is about three times the standard deviation and is thus significantly different from zero.

Among the doublets we discovered (Fig. 2) are two sets of earthquake triplets, which provide another powerful display of systematic travel time change (fig. S3). One set (triplet t1) is separated by less than 2 years; the other set (triplet t2) by 10 to 33 years. Triplet t2 includes the best recorded doublet (93 and 03) and another SSI event in 1970. The similarity of *P* waveforms at stations San Juan, Puerto Rico (SJG) and Scott Base, Antarctica (SBA), which recorded all three events, confirms that

the three events indeed occurred at the same location or nearby locations (fig. S3E). The *DF* arrival times agree well with each other in each pair of the triplet t1, but the *DF* of the later event in pairs of triplet t2 is early by 0.11, 0.24, and 0.34 s, respectively, as the time separation increases from 10, to 24, and to 33 years.

Most of our doublets were recorded at COL with clear *DF* phase (Fig. 2). Our discovery of the doublets with large time separation makes it possible to observe large time shifts in the *BC* – *DF* differential time, and the numerous doublets make it possible to characterize the uncertainty of the inferred temporal change. Figure 4 shows consistent increase of our measured $d(BC - DF)$ values at COL with time separation. The data show very small scatter, tightly constraining estimates of the rate of the temporal change (table S4). Assuming each doublet consists of colocated events, our estimate of the temporal change is 0.0092 ± 0.0004 s/year (Fig. 4). Correct-

Fig. 3. Paths within the inner core for doublet events separated by more than 4 years, all of which show a positive time shift. (A) Map view of *DF* paths projected up to the Earth's surface, including the 93 and 03 doublet, detected by 58 stations; nine additional doublets detected at the College station, Alaska; and two additional doublets detected at the Beaver Creek array. (B) Vertical cross-section *a* – *b* showing the *DF* ray turning radius. Open circles are paths to single stations, filled circles are paths to arrays in Alaska, and circle size indicates the measured time change $d(BC - DF)$ for each path, normalized to a 10-year separation. ICB, inner core boundary.

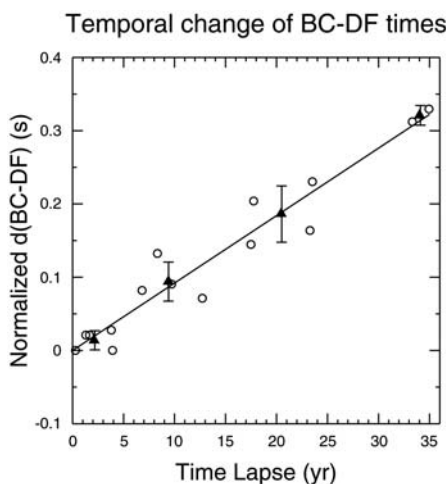
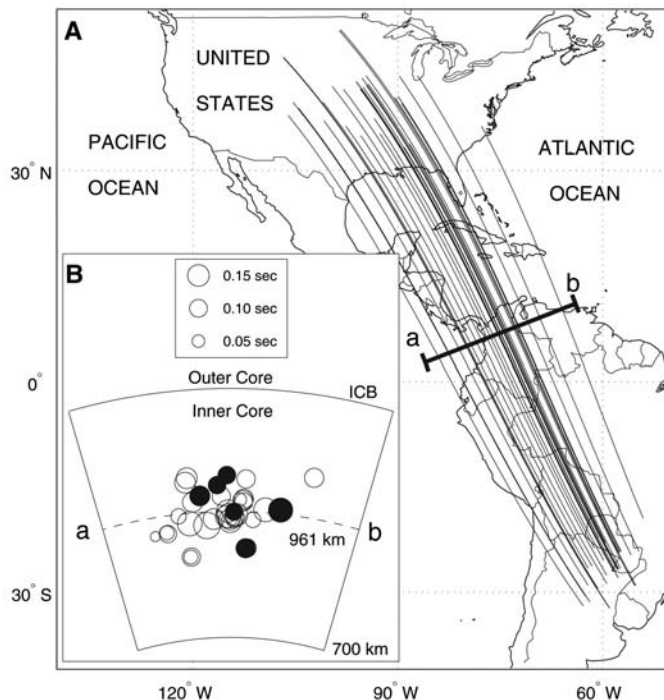


Fig. 4. Difference of *BC* – *DF* times, $d(BC - DF)$, at station COL as a function of the time separation between the two events of the doublet. The error bar indicates the mean (solid triangle) \pm SD of the data binned over a 5-year period. The measured $d(BC - DF)$ value has been normalized by the travel time through the inner core and then multiplied by the travel time through the inner core at the average distance of 151° . The line is the linear regression of the data with zero intercept; the slope is 0.0092 s/year with standard deviation 0.0004 s/year.

ing for event separation of up to a few kilometers, as indicated by the small values of $d(AB - BC)$ times (table S2), changes this result little and gives the estimated temporal change as 0.0090 ± 0.0005 s/year (fig. S9) (25). Both these new estimates are about 20 times their measurement errors, which is very strong evidence the travel time is indeed changing. They are also very close to the val-

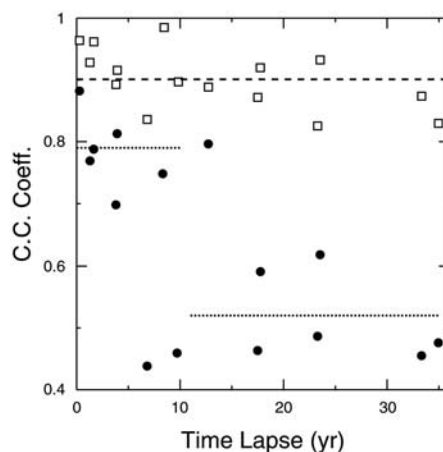


Fig. 5. Cross-correlation coefficients of the *BC* phase (open squares) and the *DF* phase and its coda (solid circles) for the doublets at station COL, as a function of the time separation between the two events of the doublet. The mean of the *BC* values is indicated by the dashed line. The *DF* values seem bimodal and the means of the two groups are indicated by the dotted line segments. The time window used to calculate the *DF* cross-correlation coefficient (C. C. Coeff.) includes the onset of the *DF* phase and its coda up to the onset of the *BC* phase.

ue first obtained by Song and Richards (4), 0.0109 ± 0.0014 s/year. Systematic temporal change is also clear from doublets at Beaver Creek array even though the time separation is much shorter (10 years) (fig. S10).

Our waveform doublets show that the waveforms of the *DF* coda become dissimilar when the time separation is larger than about 7 years (Fig. 2 and fig. S11), providing additional evidence for an inner core motion. Changes in

PKP coda ascribed to inner core rotation have been noted elsewhere (15). Figure 5 shows cross-correlation coefficients of *BC* and *DF* waveforms for each doublet at COL. The *BC* cross correlation fluctuates from 0.82 to 0.98. However, the cross correlation of the *DF* phase and its coda deteriorates sharply from about 0.79 to about 0.52 when the time separation is greater than 7 to 10 years. For doublets with large time separation, the low *DF* cross-correlation coefficients are upper bounds, as cycles may have been skipped in order to find the highest correlation. The *DF* coda is presumably caused by scattering within a complex anisotropic heterogeneous structure (27–29). So the observed breakdown of waveform similarity is evidence, independent of travel time change, for motion of the inner core.

Assuming the temporal change in *BC* – *DF* times is the result of a shift of the underlying lateral velocity gradient in the inner core due to the rotation around the spin axis (5), our new estimated rotation rate is about 0.27° to 0.53° per year (table S5). The biggest uncertainty in determining the inner core rotation rate lies not in estimating the temporal change of travel times but in imaging lateral changes of velocity within the inner core.

References and Notes

1. D. Gubbins, *J. Geophys. Res.* **86**, 11695 (1981).
2. G. A. Glatzmaier, P. H. Roberts, *Phys. Earth Planet. Inter.* **91**, 63 (1995).
3. B. A. Buffett, G. A. Glatzmaier, *Geophys. Res. Lett.* **27**, 3125 (2000).
4. X. D. Song, P. G. Richards, *Nature* **382**, 221 (1996).
5. K. C. Creager, *Science* **278**, 1284 (1997).
6. X. D. Song, *J. Geophys. Res.* **105**, 7931 (2000).
7. J. E. Vidale, D. A. Dodge, P. S. Earle, *Nature* **405**, 445 (2000).
8. X. D. Song, *Phys. Earth Planet. Inter.* **122**, 221 (2000).
9. X. D. Song, A. Y. Li, *J. Geophys. Res.* **105**, 623 (2000).
10. J. D. Collier, G. Helffrich, *Earth Planet. Sci. Lett.* **193**, 523 (2001).
11. A. Y. Li, P. G. Richards, in *Earth's Core: Dynamics, Structure, and Rotation (Geodynamics Series 31)*, V. M. Dehant, K. C. Creager, S. Zatman, S. Karato, Eds. (American Geophysical Union, Washington, DC, 2003), pp. 23–30.
12. A. Y. Li, P. G. Richards, *Geochem. Geophys. Geosys.* **4**, 10.1029/2002GC000379, 1072 (2003).
13. X. X. Xu, X. D. Song, *Geophys. J. Int.* **152**, 509 (2003).
14. G. Laske, G. Masters, in *Earth's Core: Dynamics, Structure, and Rotation (Geodynamics Series 31)*, V. M. Dehant, K. C. Creager, S. Zatman, S. Karato, Eds. (American Geophysical Union, Washington, DC, 2003), pp. 5–21.
15. J. E. Vidale, P. S. Earle, *Geophys. Res. Lett.* **32**, L01309, 10.1029/2004GL021240 (2005).
16. A. Souriau, *Geophys. J. Int.* **134**, F1 (1998).
17. A. Souriau, G. Poupinet, *Phys. Earth Planet. Inter.* **118**, 13 (2000).
18. A. Souriau, P. Roudil, B. Moynot, *Geophys. Res. Lett.* **24**, 2103 (1997).
19. A. Souriau, *Science* **281**, 55 (1998).
20. G. Poupinet, A. Souriau, O. Coutant, *Phys. Earth Planet. Inter.* **118**, 77 (2000).
21. A. Souriau, G. Poupinet, in *Earth's Core: Dynamics, Structure, and Rotation (Geodynamics Series 31)*, V. M. Dehant, K. C. Creager, S. Zatman, S. Karato, Eds. (American Geophysical Union, Washington, DC, 2003), pp. 65–82.
22. G. Poupinet, W. L. Ellsworth, J. Frechét, *J. Geophys. Res.* **89**, 5719 (1984).
23. D. P. Schaff, P. G. Richards, *Science* **303**, 1176 (2004).

24. X. D. Song, *Phys. Earth Planet. Inter.* **124**, 269 (2001).
 25. Materials and methods are available as supporting material on Science Online.
 26. F. Waldhauser, W. L. Ellsworth, *Bull. Seism. Soc. Am.* **90**, 1353 (2000).
 27. X. D. Song, X. X. Xu, *Geophys. Res. Lett.* **29**, 10.1029/2001GL013822 (2002).
 28. J. E. Vidale, P. S. Earle, *Nature* **404**, 273 (2000).
 29. V. F. Cormier, X. Li, *J. Geophys. Res.* **107**, 10.1029/2002JB001796 (2002).
 30. We thank the Data Management Center of the Incorporated Research Institutions for Seismology and the Alaska Seismic Network for making the data openly accessible. Digital data from the U.S. Atomic Energy Detection System stations were provided by the Air Force Tactical Applications Center. X.S. thanks J. Bass for discussion. This work was supported by the NSF and by the Natural Science Foundation of China. This is Lamont-Doherty Earth Observatory contribution number 6807.

Supporting Online Material
www.sciencemag.org/cgi/content/full/309/5739/1357/DC1
 Materials and Methods
 Figs. S1 to S11
 Tables S1 to S5
 References

5 April 2005; accepted 20 July 2005
 10.1126/science.1113193

Carbon Flux and Growth in Mature Deciduous Forest Trees Exposed to Elevated CO₂

Christian Körner,^{1*} Roman Asshoff,¹ Olivier Bignucolo,¹ Stephan Hättenschwiler,^{1,2} Sonja G. Keel,³ Susanna Peláez-Riedl,¹ Steeve Pepin,^{1,4} Rolf T. W. Siegwolf,³ Gerhard Zotz¹

Whether rising atmospheric carbon dioxide (CO₂) concentrations will cause forests to grow faster and store more carbon is an open question. Using free air CO₂ release in combination with a canopy crane, we found an immediate and sustained enhancement of carbon flux through 35-meter-tall temperate forest trees when exposed to elevated CO₂. However, there was no overall stimulation in stem growth and leaf litter production after 4 years. Photosynthetic capacity was not reduced, leaf chemistry changes were minor, and tree species differed in their responses. Although growing vigorously, these trees did not accrete more biomass carbon in stems in response to elevated CO₂, thus challenging projections of growth responses derived from tests with smaller trees.

How forest trees, the largest biomass carbon (C) pool on Earth, will respond to the continued rise in atmospheric CO₂ is unknown (1). Is there a potential for more growth, and perhaps more C storage, as a result of CO₂

fertilization (2)? Are trees in natural forests already carbon saturated, given that CO₂ concentrations have already reached twice the glacial minimum concentration (3)?

Experimental ecology has made important advances in recent years answering such questions, but unlike grass and shrub vegetation, adult forest trees do not fit any conventional test system with elevated CO₂. Free air CO₂ enrichment (FACE) is currently applied to fast-growing plantations (4–7), but to date, tall trees in a natural forest have not been studied because of overwhelming technical difficulties. We solved this problem with a technique called web-FACE (8) that releases pure CO₂ through a fine web of tubes woven into tree

canopies with the help of a construction crane (Fig. 1) (9). Here, we present responses of 32- to 35-m-tall trees in a near-natural deciduous forest in Switzerland (9) to a 530 parts per million (ppm) CO₂ atmosphere over 4 years. Given the size and species diversity of the study trees, this project inevitably is tree- and not ecosystem-oriented, in contrast to other FACE projects, which use smaller trees. Because plant responses to CO₂ are species-specific (10, 11), insight from single-species approaches remains limited, no matter how large the test scale. The statistical power of our approach is limited at the species level because of reduced intraspecific replication, but tree-ring analysis helps to account for much of the variation in tree vigor. The ultimate effect of rising CO₂ will remain concealed within our limited time scales, yet knowing the dynamics of tree responses over a number of years helps to estimate the nonlinear, longer-term trends. The project is thus a compromise between realism and precision, given that there is no way to maximize both (12).

Web-FACE uses CO₂ gas with a constant carbon isotope composition (δ¹³C) of −29.7 ± 0.3‰ (mean ± SE of four annual means). Mixture with ambient-air CO₂ (δ¹³C = −8‰) results in a ¹³C tracer signal in photoassimilates that was monitored at ~50 canopy positions with “iso-meters” (small containers planted with a grass using the C₄ photosynthetic pathway), which yielded a 4-year mean of 5.8 ± 0.5‰ ¹³C tissue depletion. Once assimilated by leaves, the signal penetrates the various biomass compartments and allows one to track the fate of carbon. During the first season, leaves accreted 40% (*Quer-*

¹Institute of Botany, University of Basel, Schönbeinstrasse 6, CH-4056 Basel, Switzerland. ²Center of Functional Ecology and Evolution, CEFE-CNRS, 1919, route de Mende, F-34293 Montpellier cedex 5, F-34293 France. ³Laboratory of Atmospheric Chemistry, Paul Scherrer Institute, CH-5232 Villigen PSI, Switzerland. ⁴Faculté des sciences de l'agriculture et de l'alimentation, Pavillon Paul-Comtois, Université Laval, Québec (Qc) G1K 7P4, Canada.

*To whom correspondence should be addressed. E-mail: ch.koerner@unibas.ch

Fig. 1. Canopy CO₂ release by a web of porous tubes (left), with “iso-meters” (front) and gas sampling lines (back) for control, all operated from a 45-m-high crane (right).

